



● *Original Contribution*

A SENSITIVE NEW INDICATOR FOR DIAGNOSTICS OF OVARIAN MALIGNANCY, BASED ON THE DOPPLER VELOCITY SPECTRUM

YODFAT SHAHARABANY,* SOLANGE AKSELROD* and RONNIE TEPPER[†]

*Abramson Center for Medical Physics, Tel-Aviv University, Tel Aviv, Israel; and [†]Ultrasound Unit, Department of Obstetrics and Gynecology, Sapir Medical Center, Kfar-Saba, Israel

(Received 10 April 2003; revised 16 October 2003; in final form 23 October 2003)

Abstract—Ovarian cancer is the most deadly gynecological malignancy, with an overall survival rate of about 35%. Approximately 60% of the cases of ovarian cancer are lethal. Ultrasonic examination, including Doppler imaging, is a commonly used technique for the diagnosis of ovarian masses. Two major clinical parameters, currently derived from the Doppler flow waveform, are the resistance index (RI) and the pulsatility index (PI). The decay constant of the Doppler waveform, which characterizes its decrease from systole to diastole as an exponential decay, has recently been presented as an additional measure of tumor malignancy. In this paper, we have analyzed the velocity spectrum of the Doppler flow signal to determine if it reveals differences that might contribute to the diagnosis of malignancy. We designed a new parameter characterizing the slope of the mean velocity spectrum at end-diastole (“End Diastolic Velocity Distribution Slope,” referred to as DVD_S). Additional indices, related to various approaches for the analysis of the Doppler image, were also derived. However, they proved to be inferior to the DVD_S. The DVD_S was tested on 20 benign and 33 malignant ovarian images. This new parameter seems to provide a good ability to discriminate between the two types of tumor. Its mean value is 1.90 ± 1.33 for malignant tumors, compared to 9.21 ± 5.34 for benign masses (area under ROC curve: 0.983), yielding a detection rate of about 94%. In fact, this parameter provides much better results than the previously used variables, and has the potential to significantly improve the detection of malignancy. (E-mail: solange@post.tau.ac.il) © 2004 World Federation for Ultrasound in Medicine & Biology.

Key Words: Ovarian masses, Doppler flow images, Velocity spectrum, Malignancy evaluation, Image processing.

INTRODUCTION

Ovarian cancer is the sixth most common cancer in women, and the second most common gynecological malignancy. Of the newly detected cases, 70% are typically already in advanced stages (Taylor and Schwartz 1994). Unfortunately, whether benign or malignant, ovarian tumors rarely produce specific symptoms, and there are no diagnostic criteria sensitive enough to discriminate between the two at an early stage of the disease. Late detection is one of the major reasons why ovarian cancer is a more lethal disease than any other reproductive organ cancer.

One of the commonly used techniques for the diagnosis of ovarian masses is ultrasonic examination, including Doppler imaging. The two major parameters that, in the clinical setting, are currently extracted from the Doppler flow waveform are the resistance index (RI)

and the pulsatility index (PI) (Maulik 1997). The decay constant of the descending part of the Doppler waveform has recently been demonstrated to be an additional measure for the malignancy of the tumor (Tepper et al. 1997). This parameter was also used for flow analysis in the carotid artery to quantify the Windkessel function of elastic arteries (Nagai et al. 1999, 2001). In these approaches, the ultrasound (US) Doppler image is considered essentially as a 2-D image.

The purpose of this study was to develop new parameters that have high discrimination capacity, and can eventually be used to discriminate between benign and malignant ovarian tumors. As a first step, we calculated an improved version of the decay constant (Tau), by averaging the decay constant over several waveforms, using weights. These weights were determined by the quality of the exponential fit, performed on each flow waveform in the Doppler signal.

However, we noticed that using only parameters derived from the 2-D Doppler flow waveform does not discriminate sufficiently between benign and malignant

Address correspondence to: Solange Akselrod, Ph.D., Abramson Center for Medical Physics, Tel Aviv University, Tel Aviv 69978 Israel. E-mail: solange@post.tau.ac.il

tumors. We, therefore, chose to examine the entire velocity spectrum, considering the Doppler flow image as a 3-D image, which displays the velocity histogram as a function of time. We developed four additional parameters (further detailed below); two parameters (ADD, MAV) were based on computing the weighted average velocities, and the other two (BPA, mH2L) were derived from plotting the entire velocities spectra at all times considered. This new approach consisting of 3-D analysis, enabled better discrimination between benign and malignant tumors, and motivated us to extend the investigation established on the 3-D approach.

The blood volume flow is linearly proportional to the pressure drop in the vessel (caused by the cardiovascular activity) and extremely dependent on its radius, as clearly expressed in Poiseuille's equation. During diastole, the pressure drop is very low and the flow is mainly affected by the vessel diameter. The ability of the vessel to contract, hence, reducing its volume, is affected by the characteristics of the smooth muscle in the vessel walls.

Angiogenesis, the process of generating new capillaries from pre-existing blood vessels, is essential for the growth of solid tumors. Angiogenesis is accelerated when the tumor cells release a diffusible chemical substance that disturbs the balance between angiogenesis stimulators and inhibitors (Folkman 1976). The newly formed capillaries grow toward the tumor, covering it from all directions, and penetrate it. Therefore, tumor microvasculature does not conform to the vasculature of healthy tissues. The angiogenesis process that can be found within ovarian tumors includes giant capillaries that are leaky to plasma proteins and contain fewer smooth muscle cells in their walls (Dvorak et al. 1988), resulting in a reduced contractile capability. Owing to this poorly developed muscular coat in malignant tumor vessels, the flow waveform signals are characterized by low impedance shunts (Emoto et al. 1997).

Based on the different physiological features of the blood vessels in patients with tumors, we searched for additional parameters that might characterize the elasticity of the blood vessels. We, therefore, analyzed the shape of the velocity spectrum at two specific time intervals, focusing on its slope; after end-systole (SVD_S), and before end-diastole (DVD_S).

Our goal in this study was to design one or more new parameters based on the shape of the Doppler blood flow velocity spectrum, that might serve as a sensitive discriminator of ovarian malignancy.

METHODS

Data acquisition

This study included postmenopausal patients with ovarian mass, who were under medical evaluation at the

Sapir Medical Center Ultrasound Unit, Gynecological Department. Inclusion criteria were: 1. histologically confirmed ovarian tumor, 2. ovarian mass evaluated by Doppler US at the time of the TVS (transvaginal sonography) examination, 3. all TVS and recorded Doppler flow examinations followed by histopathological analysis in the same patients were included in the research.

TVS and Doppler were performed using a US system equipped 128XP10 (Acuson, Mountain View, CA, USA) with high-resolution endovaginal transducer 5–7 MHz.

The study involved the quantitative analysis of 53 US Doppler images from postmenopausal patients with ovarian masses; 33 images of malignant tumors and 20 images of benign ones. All tumors were examined histologically according to the World Health Organization classifications.

The images were recorded on video cassettes and later digitized into the computer using a DT-2853 frame grabber (Data Translation, Marlboro, MA, USA), yielding images containing 512 pixels \times 512 pixels \times 256 grey levels.

The Doppler images were submitted to an algorithm for velocity spectrum analysis, developed on a personal computer (PC), based on Matlab 6.0.

Flow analysis

The algorithm for velocity spectrum analysis consists of several steps. To perform the waveform delimitation, the Doppler flow image was smoothed by a median filter with a window size of 11 \times 11 pixels. Figure 1 displays automatically extracted contours for a single wave before and after smoothing.

The Doppler flow image can be regarded as a 3-D image, with time axis, velocity axis, and grey-level distribution. The grey level of each pixel is proportional to the number of the red blood cells, passing through the blood vessel at a specific time and velocity. An instantaneous spectrum of velocities is, thus, displayed as a function of time. Each pixel on the time axis corresponds approximately to 11.4 ms.

To achieve an improved discrimination between benign and malignant tumors, we developed an algorithm that enables us to compute several new parameters describing the features of the velocity spectrum. We divided the instantaneous flow spectrum into two parts: all the velocities with values higher than the minimal end diastolic velocity in the image were considered as "high velocities," and all the values below that were defined as "low velocities" (Fig. 2).

Figure 3a displays an example of the velocity spectrum at two specific instants in time, while Fig. 3b displays all the successive velocity spectra obtained as a function of time for several consecutive cardiac beats. A

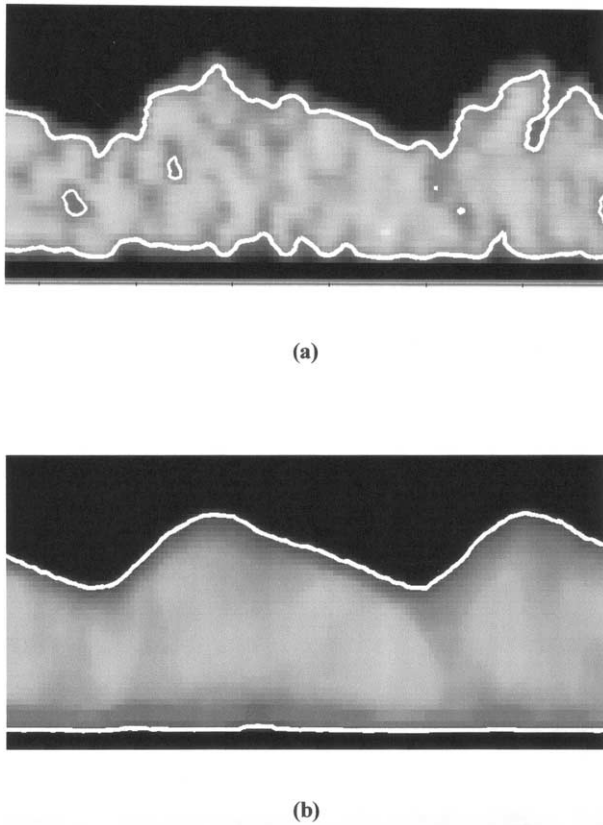


Fig. 1. Automatically extracted contours for one wave in the Doppler flow image, (a) without filtering and, (b) after smoothing by median filter 11×11 .

line is drawn for the velocity spectrum at each time unit in a sequence of a few beats. Figure 3c shows only the part of the velocity spectrum referred to in this study as “high velocities” (*i.e.*, the velocity range above the end diastolic velocity).

In Fig. 3a to d, the y-axis represents the probability of occurrence of each velocity (*i.e.*, the grey levels 0 to 255 normalized to the range 0–1). The x-axis represents the velocity on an arbitrary scale. Each curve in this figure reflects a different instant in time. In other words,

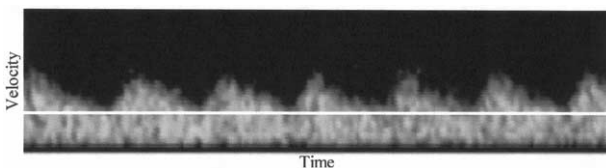


Fig. 2. Doppler flow image. The white line represents the minimal end diastolic velocity. All the velocities with values higher than the minimal end diastolic velocity are regarded as “high velocities,” and all the values below that velocity, as “low velocities.”

a point on one of the curves displayed in Fig. 3 reflects the probability of finding a specific velocity at the time instant represented by that curve.

We plotted the successive velocity spectra of the Doppler flow waveform for several consecutive beats (Fig. 3b), and calculated the maximum occurrence curve (*i.e.*, the maximal occurrence for each velocity at all times) and the average spectrum curve (*i.e.*, the average occurrence for each velocity at all times).

From the analysis of the velocity spectrum, several quantitative parameters were designed and extracted. Among those are the “mean High2Low” (mH2L) parameter and the “break point angle” (BPA). The mH2L is computed on the mean curve of the velocity spectra at all times (Fig. 3b, cyan curve), and is defined as the ratio between the area under the curve in the “high-velocity” range to the area under the curve in the “low-velocity” range. The BPA (Fig. 3d) is computed in the “high velocities” range, at maximum probability along the envelope of the velocity spectrum, and defined as the angle (β) between two lines; the first line is a linear fit to the 40% of the left end of the maximum occurrence curve, and the second line is a linear fit to the 40% of the right end of the curve.

Two additional parameters were designed after normalizing the velocities to the range 0–1; The “Minimal Average Velocity” (MAV), which is the minimum average velocity per all times (Fig. 4b), and the “Average Difference in Diastole” (ADD), calculated at the end diastolic time instants over a sequence of several beats. For every end diastolic time instant, we calculated the weighted average velocity, with the grey levels (probabilities of occurrence for each velocity) as the weights. The ADD is the mean value (over several beats) of the differences between the end diastolic maximum velocities, and the weighted average velocities at the end diastolic times (Fig. 4a).

In addition, the physiological behavior of the blood vessels prompted us to analyze the velocity spectrum at two specific time intervals: immediately after the end systolic peak, where we expect maximum influence of the heart on the blood flow, and before end diastole, where we expect minimum effect of the heart and maximum expression of the blood vessel characteristics.

Each of these two intervals was chosen to be 6 pixels wide, which is about 10% of the duration of a single wave (Fig. 5).

We plotted the mean curve of each spectrum obtained at the “low velocities” part, (*i.e.*, the mean curves at the end diastolic velocity spectrum and the end systolic velocity spectrum) and calculated its slope by performing a linear fit. The slopes for the end diastole and for the end systole will, henceforth, be called DVD_S (as for “end Diastolic Velocity Distribution Slope”) and

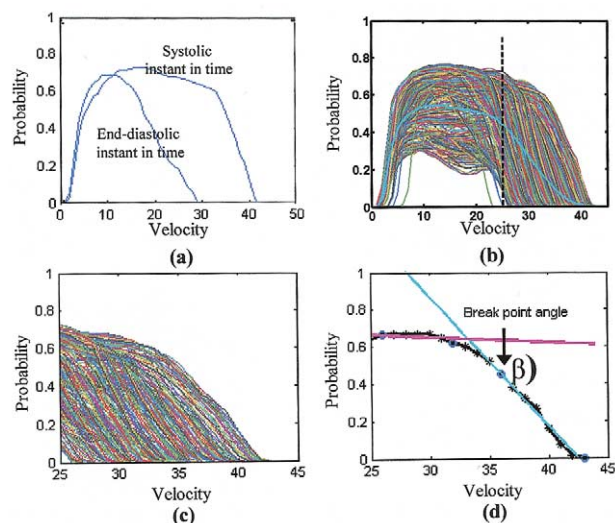


Fig. 3. The velocity spectrum and the BPA. (a) Example for two velocity spectra at a systolic and an end diastolic instant of time (selected randomly). (b) All velocity spectra at all times. The mean curve is shown in cyan; the black dashed line divides between the “high-velocity” range (on its right) and the “low-velocity” range (on its left). (c) Zooming into the high-velocity range only. (d) The BPA is the angle (β) between the magenta line and the cyan line.

SVD_S (“Systolic Velocity Distribution Slope”), respectively.

Figure 6a and b shows the curves of the end diastole velocity spectra in benign and malignant Doppler flow images, respectively. The different curves in Fig. 6a and b represent the velocity spectrum at different times during the end diastolic time intervals.

Figure 6c and d display the mean curve and its linear fit for the end diastolic velocity spectra in the benign and the malignant cases, respectively.

The linear fit (namely, least squares) was performed

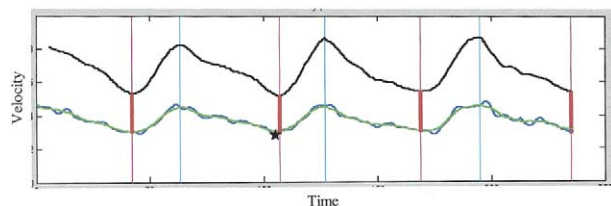


Fig. 4. Mean velocity curves, calculated as a weighted average on a filtered (green) and not-filtered (blue) Doppler flow image. The black curve shows the maximal velocities at all times. The systolic (cyan) and the end-diastolic (pink) time instants are displayed. The red streaks are the differences between the maximal velocities and the mean velocities at the end diastolic time instants. Their mean value is the ADD. The MAV (black pentagram) is the minimal average velocity in the entire time range.

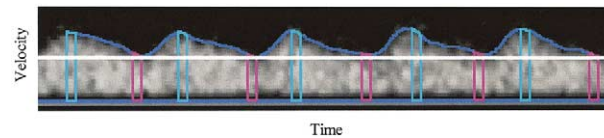


Fig. 5. Extracting the parameter DVD_S. Systolic and end diastolic time intervals are plotted in cyan and pink 6-pixel wide frames, respectively. SVD_S and DVD_S were extracted from these interval at the “low velocities” part (the area under the white line).

only for the main part of the mean velocity distribution curve, after discarding the leftmost 20% of the curve and, in rare cases, the fast falling part at its right end. The left end of the curve (*i.e.* the values at low velocities) does not reflect real probabilities, but false values resulting from a high-pass filter procedure performed automatically by the US device on the Doppler signals. This high-pass filtering is performed for the purpose of eliminating extrinsic low-frequency (velocity) components, which arise predominantly from the vessel walls or other adjacent slow-moving structures.

In some cases, the right end of the curve (*i.e.*, the distribution values at high velocities) contains very small probability values that result from setting a shifted maximum waveform curve. This shift is due to a corresponding shift at the automatically extracted contour, used for deriving the maximum waveform curve. In case the latter

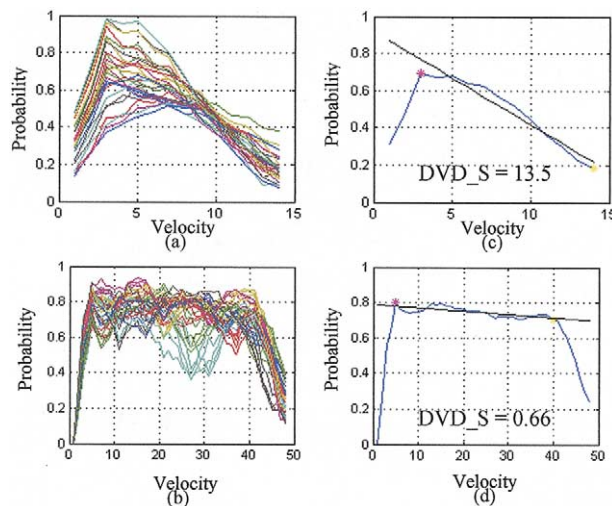


Fig. 6. The DVD_S parameter produced from benign ((a) and (c)) and malignant ((b) and (d)) images. (a) and (b) show the velocity spectrum curves during end diastolic time intervals, in benign and malignant images, respectively. (c) and (d) show the velocity spectrum mean curves during end diastolic time intervals, and their linear fits. In (c), the linear fit was obtained on the descending part of the curve, while in (d) the linear fit was obtained on the plateau part of the curve.

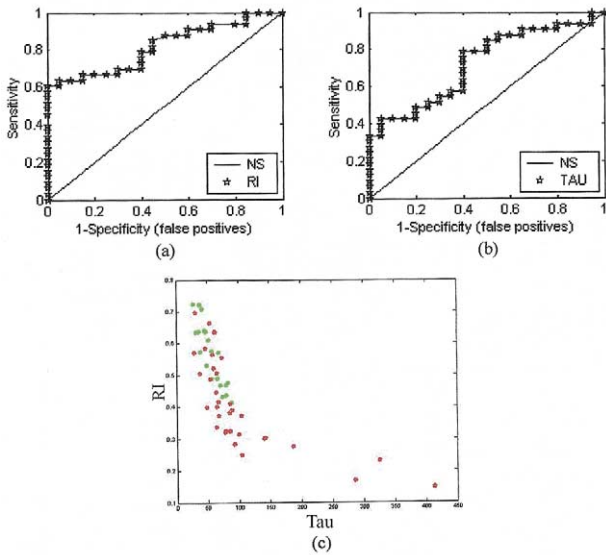


Fig. 7. ROC curves drawn for (a) RI and (b) Tau. (c) is a plot of RI vs. Tau. The red stars represent malignant tumors, while the green stars represent benign ones. Obviously, there is no good separation between malignant and benign.

shift is upward, the automatic contour is drawn above the boundary layer between the actual wave and the background. Because this layer represents velocities higher than the real maximum ones in the wave, these values should be discarded. Figure 6d demonstrates a curve in which the left end (lower velocities) and the right end (higher velocities) were discarded.

The slopes of these linear fits (Fig. 6c and d) are the end-Diastolic Velocity Distribution Slopes, hence called the DVD_S.

RESULTS

The values obtained for the standard Doppler velocity parameters are as follows: RI was 0.40 ± 0.14 for malignant tumors and 0.56 ± 0.10 for benign masses.

The new version (the weighted one) of the decay constant (Tau) was 108 ± 81 for malignant tumors, and 57 ± 18 for benign masses. A receiver operating characteristic (ROC) curve was drawn for each parameter; the area under the ROC curve was 0.816 ($p < 0.0001$) for RI, and 0.723 ($p = 0.0008$) for Tau. Figure 7a and b displays the ROC curves of RI and Tau, respectively. Figure 7c displays Tau vs. RI for our data set.

The display of RI vs. Tau (Fig. 7c) shows no significant separation between benign (green) and malignant (red) masses; many data points do overlap.

The parameters produced by the 3-D analysis of the velocity spectrum as a function of time, reached the following values:

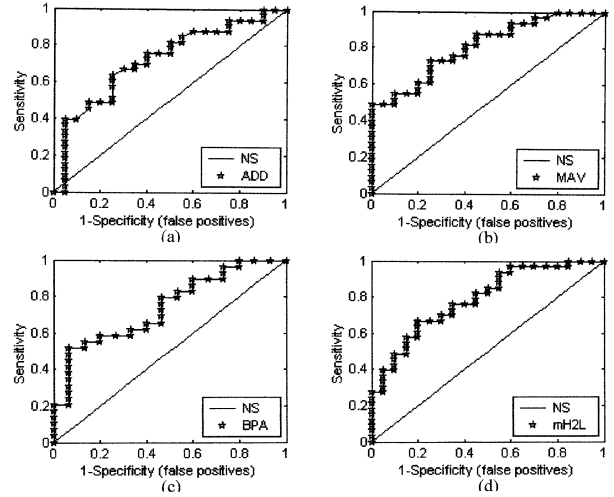


Fig. 8. ROC curves drawn for (a) ADD, (b) MAV, (c) BPA and (d) mH2L.

- The ADD was 0.22 ± 0.07 for malignant tumors, and 0.14 ± 0.07 for benign masses. The area under the ROC curve was 0.723 ($p = 0.0011$).
- The MAV was 0.24 ± 0.06 for malignant tumors, and 0.17 ± 0.04 for benign masses. The area under the ROC curve was 0.808 ($p < 0.0001$).
- The BPA was $17 \pm 18^\circ$ for malignant tumors, and $32 \pm 33^\circ$ for benign masses. The area under the ROC curve was 0.740 ($p = 0.0009$).
- The mH2L was 0.38 ± 0.21 for malignant tumors and 0.69 ± 0.34 for benign masses. The area under the ROC curve was 0.786 ($p < 0.0001$).

Figure 8 displays the ROC curves of these parameters.

Figure 9 displays plots of various pairs of these parameters.

Although it seems that adding these new parameters improves (see Fig. 9c or d) the discrimination between benign and malignant tumors, the overlap is still significant and, therefore, the discrimination result is still not satisfactory.

Table 1. Performance of DVD_S

Threshold	Specificity (%)	Sensitivity (%)	NPV (%)	PPV (%)	Success rate (%)
3.5	100	91	87	100	94
4	95	91	86	97	92
4.5	95	94	90	97	94
5	90	97	95	94	94

PPV = positive predictive value; NPV = negative predictive value.

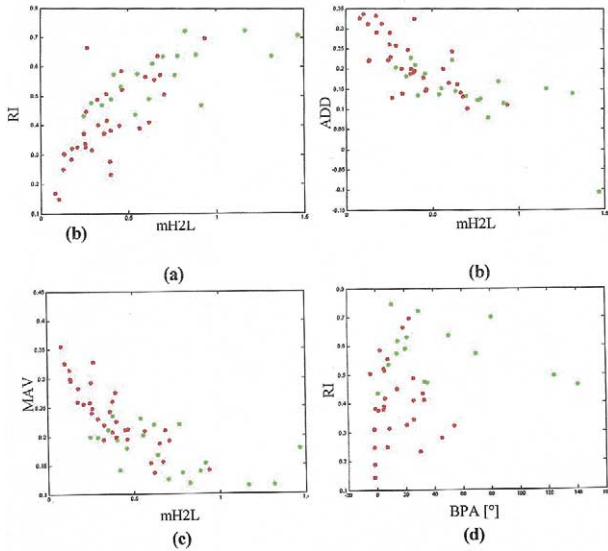


Fig. 9. (a) RI vs. mH2L, (b) ADD vs. mH2L, (c) MAV vs. mH2L, (d) RI vs. BPA (red and green, as in Fig. 7c).

The values obtained for the other two parameters (DVD_S and SVD_S), extracted from the 3-D analysis of the velocity spectrum in specific time intervals (end diastole and systole), are as follows. The DVD_S was 1.90 ± 1.33 for malignant tumors and 9.21 ± 5.34 for benign masses. The area under the ROC curve was 0.983 ($p < 0.0001$). The SVD-S was 0.97 ± 1.38 for malignant tumors and 1.46 ± 4.57 for benign masses. The area under the ROC curve was 0.507 ($p = 0.4727$, NS as expected). Figure 10 displays the ROC curves of these parameters.

To assess the performance of the DVD_S, we classified a set of 53 images (33 malignant, 20 benign) using only the values of this parameter. The results are presented in Table 1. In this table, each row refers to discriminating between malignant tumors and benign ones, using a different value of DVD_S as a threshold (for 3.5 to 5).

Figure 11 displays RI, ADD, and combined RI and Tau vs. the end diastolic slope (DVD_S). The discrimi-

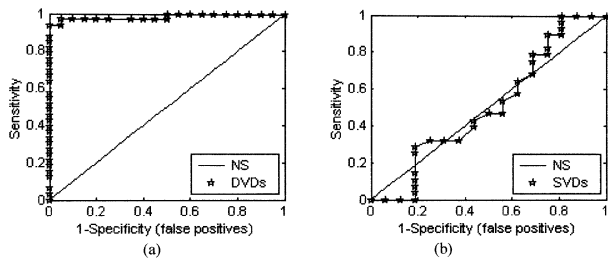


Fig. 10. ROC curves drawn for (a) DVD_S and (b) SVD_S.

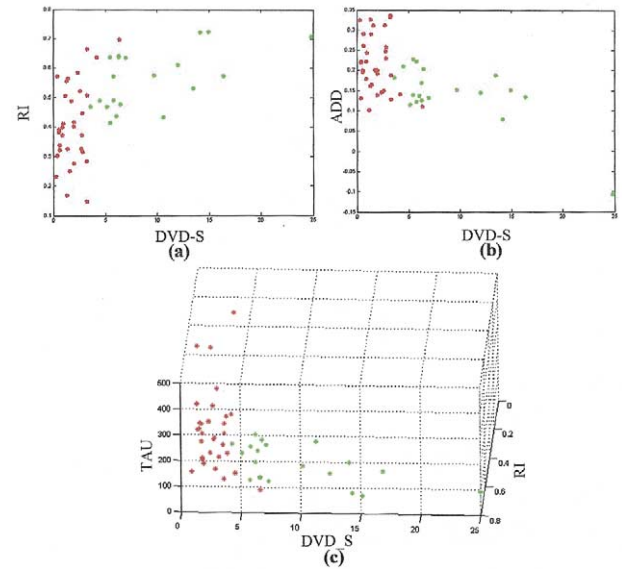


Fig. 11. Several parameters plotted vs. the end Diastolic Velocity Distribution Slope. (a) RI vs. DVD_S, (b) ADD vs. DVD_S, (c) 3-D plot of Tau and RI vs. DVD_S.

nation of benign and malignant tumors into separate clusters is evident, as opposed to the inadequate separation attained by the previously defined parameters (compare with Figs. 7 and 9).

It is clear that DVD_S achieves a much better discrimination.

A summary of the values obtained for all the parameters is presented in Table 2.

The results obtained for DVD_S are evidently promising, and indicate that the DVD_S has a good chance of being a suitable parameter for the evaluation of malignancy.

DISCUSSION

In this study, we developed a new approach to the analysis of Doppler images. We regarded the Doppler flow image as a 3-D image, and examined the entire

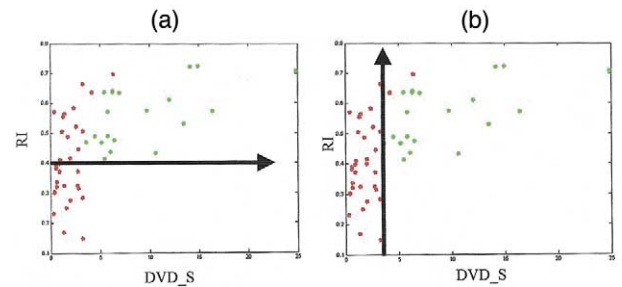


Fig. 12. Malignancy classifications by (a) RI and (b) DVD_S.

Table 2. Summary of all the results

Parameter	Malignant tumors		Benign masses		ROC curve	
	Average	Std.	Average	Std.	Area under	<i>p</i>
RI	0.40	0.14	0.56	0.10	0.816	<0.0001
Tau	108	81	57	18	0.723	0.0008
BPA	17	18	32	33	0.740	0.0009
mH2L	0.38	0.21	0.69	0.34	0.786	<0.0001
MAV	0.24	0.06	0.17	0.04	0.808	<0.0001
ADD	0.22	0.07	0.14	0.07	0.723	0.0011
DVD_S	1.90	1.33	9.21	5.34	0.983	<0.0001
SVD_S	0.97	1.38	1.46	4.57	0.507	NS

velocity spectrum as a function of time. This new approach enabled us to design new parameters that provided interesting results regarding the discrimination among ovarian masses, and can supply a solid ground for in-depth analysis.

Some of the parameters extracted from the entire velocity spectrum (3-D) achieved better results than the decay constant that was generated from the 2-D Doppler waveform. We also found that the separation capacity between benign and malignant tumors was significantly influenced by the selection of the time intervals in which these parameters were computed.

We hypothesized that the end diastolic measurement will prove to be the best because it minimizes the effect of cardiac contractility and emphasizes the vascular effect on blood flow; thus, stressing the difference in the flow characteristics related to ovarian malignancy. As expected, we found in our study that parameters obtained mainly from the end diastolic range achieved better discrimination than those generated on the entire velocity spectrum. For example, the separation capacity between benign and malignant tumors using the end systolic parameter (*i.e.*, SVD_S), which is more strongly influenced by cardiac function, was very poor. However, the end diastolic parameter (*i.e.*, DVD_S) seems to offer an extremely sensitive discrimination ability between the two types of tumors. In fact, this parameter provides much better results than any of the previously examined variables, and markedly improves the detection of malignancy.

The major parameter currently in use for detecting malignancy by US Doppler flow measurement (*i.e.*, RI), is shown vs. our new parameter DVD_S in Fig. 12. It is obvious that, for values higher than 0.4, RI classifies a considerable number of malignant tumors as benign ones.

The newly developed parameter DVD_S classifies not only the malignant tumors with $RI < 0.4$ in particular but, actually, most of the images with a much greater sensitivity.

Examining the results obtained for the area under the ROC curves, we found that SVD_S failed (area 0.507)

and showed no discrimination ability (as expected); Tau, BPA, mH2L and ADD showed “fair” discrimination ability (areas between 0.7–0.8), MAV and the currently used parameter RI achieved good discrimination ability (areas between 0.8–0.9), and DVD_S is far ahead with an excellent discrimination ability (area 0.983).

In our opinion, the main reason for the only “fair” discrimination ability of mH2L and BPA, is that they both were obtained by analyzing the entire velocity spectrum at all times along the heartbeats. In the future, every wave from systole to end diastole should be divided into a number of time intervals, so that the calculation of mH2L and BPA would be performed on each interval separately, resulting in a vector of numbers (for each parameter). The time evolution of these parameters and their ability to discriminate can then be investigated in detail.

In addition, ADD, mH2L, BPA and DVD_S were obviously affected by the approximation of setting one straight line to separate the “high” from the “low” velocities. This line was determined according to the minimal end diastolic velocity.

The parameter DVD_S did achieve excellent discrimination, and may become a suitable indicator of malignancy along with other diagnostic parameters currently in use for early detection of ovarian cancer. The discriminative power of DVD_S should be further validated using a larger number of clinical cases, under varying physiological conditions.

SUMMARY

Ovarian cancer is an extremely lethal disease in women, mainly because of its typically late detection. The current techniques for the diagnosis of ovarian masses do not provide satisfactory solutions for its early detection. In our study, we examined a new approach, considering the Doppler flow image as a 3-D image. We designed several new parameters, based on the analysis of the velocity spectrum of the Doppler wave flow.

The most promising parameter was the DVD_S, which characterizes the slope of the mean velocity spec-

trum around end diastole. This variable provides a success rate of malignancy detection of about 94%. In combination with other clinical parameters, it may become a suitable marker for malignancy evaluation. The performance of the proposed parameter for the early detection of malignancy should be validated using a large number of clinical cases.

Acknowledgments—The authors thank Dr. Yair Zimmer for his generous assistance. This research was supported by a grant from the Israeli Cancer Association, and also by the Abramson Foundation for Medical Physics.

REFERENCES

- Dvorak HF, Nagy JA, Dvorak JT, Dvorak AM. Identification and characterization of the blood vessels of solid tumors that are leaky to circulating macromolecules. *Am J Pathol* 1988;133:95–109.
- Emoto M, Iwasaki H, Minura K, Kawarabayashi T, Kikuchi M. Differences in the angiogenesis of benign and malignant ovarian tumors, demonstrated by analyses of color Doppler ultrasound, immunohistochemistry, and microvessel density. *Cancer* 1997;80:899–907.
- Folkman J. The vascularization of tumors. *Sci Am* 1976;234:59–73.
- Maulik D. Doppler ultrasound in obstetrics & gynecology, 1st ed. Berlin: Springer-Verlag, 1997.
- Nagai Y, Helweggen J, Fleg JL, et al. Decay index: A new carotid Doppler waveform measure associated with the windkessel function of elastic arteries. *Ultrasound Med Biol* 1999;25:1371–1376.
- Nagai Y, Helweggen J, Fleg JL, et al. Associations of aortic windkessel function with age, gender and cardiovascular risk factors. *Ultrasound Med Biol* 2001;27:1207–1210.
- Taylor KJ, Schwartz PE. Screening for early ovarian cancer. *Radiology* 1994;192:1–10.
- Tepper R, Keselbrener L, Manor M, et al. Decay constant of Doppler flow waveform as a possible indicator of ovarian malignancy. *Ultrasound Med Biol* 1997;23:1171–1177.